

Elevator, Escalator or Neither? Classifying Pedestrian Conveyor State Using Inertial Navigation System

Tianlang He Zhiqiu Xia S.-H. Gary Chan
theaf@cse.ust.hk, zxiaae@connect.ust.hk, gchan@cse.ust.hk
The Hong Kong University of Science and Technology
Hong Kong, China

ABSTRACT

Classifying a pedestrian in one of the three *conveyor states* of "elevator," "escalator" and "neither" is fundamental to many applications such as indoor localization and people flow analysis. We estimate, for the first time, the pedestrian conveyor state given the inertial navigation system (INS) readings of accelerometer, gyroscope and magnetometer sampled from the phone. Our problem is challenging because the INS signals of the conveyor state are coupled and perturbed by unpredictable arbitrary human actions, confusing the decision process. We propose ELESON, a novel, effective and lightweight INS-based deep learning approach to classify whether a pedestrian is in an **elevator**, **escalator** or **neither**. ELESON utilizes a motion feature extractor to decouple the conveyor state from human action in the feature space, and a magnetic feature extractor to account for the speed difference between elevator and escalator. Given the results of the extractors, it employs an evidential state classifier to estimate the confidence of the pedestrian states. Based on extensive experiments conducted on twenty hours of real pedestrian data, we demonstrate that ELESON outperforms significantly the state-of-the-art approaches (where combined INS signals of both the conveyor state and human actions are processed together), with 15% classification improvement in F1 score, stronger confidence discriminability with 10% increase in AUROC (Area Under the Receiver Operating Characteristics), and low computational and memory requirements on smartphones.

CCS CONCEPTS

• **Human-centered computing** → **Ubiquitous and mobile computing systems and tools**.

KEYWORDS

Pedestrian conveyor states, inertial navigation system, causal representation learning, uncertainty estimation, evidence theory

ACM Reference Format:

Tianlang He Zhiqiu Xia S.-H. Gary Chan. 2018. Elevator, Escalator or Neither? Classifying Pedestrian Conveyor State Using Inertial Navigation System. In *Proceedings of Make sure to enter the correct conference title from*

Permission to make digital or hard copies of all or part of this work for personal or classroom use is granted without fee provided that copies are not made or distributed for profit or commercial advantage and that copies bear this notice and the full citation on the first page. Copyrights for components of this work owned by others than the author(s) must be honored. Abstracting with credit is permitted. To copy otherwise, or republish, to post on servers or to redistribute to lists, requires prior specific permission and/or a fee. Request permissions from permissions@acm.org.
Conference acronym 'XX, June 03–05, 2018, Woodstock, NY

© 2018 Copyright held by the owner/author(s). Publication rights licensed to ACM.
ACM ISBN 978-1-4503-XXXX-X/18/06
<https://doi.org/XXXXXXXX.XXXXXXX>

your rights confirmation email (Conference acronym 'XX). ACM, New York, NY, USA, 10 pages. <https://doi.org/XXXXXXXX.XXXXXXX>

1 INTRODUCTION

We study, for the first time, how to classify a pedestrian in one of the three *conveyor states* of "elevator," "escalator" and "neither," given the inertial navigation system (INS) readings from accelerator (i.e. acceleration), gyroscope (i.e. angular velocity) and magnetometer (i.e. magnetic fields) sampled from the pedestrian's phone. Our problem is fundamental to many applications such as indoor localization, people flow analysis and venue design/optimization [1–5].

Our problem is challenging because the INS signals of conveyor state are coupled and perturbed by unpredictable, arbitrary and diverse human actions. Such entanglement leads to noise, and hence confusion, in the decision process. Though impressive amount of work has been done on human action recognition (HAR) [6–10], they train and infer by considering the INS signals as an aggregate. In reality, many human actions, such as walking and texting, are largely independent of the conveyor state. As these actions impact INS readings, including them in the classification process results in unsatisfactory accuracy (validated in our experiment section later).

We propose ELESON, a novel lightweight INS-based deep learning approach to classify a pedestrian is in **elevator**, **escalator**, or **neither**. ELESON achieves its effectiveness by decoupling the conveyor state from human actions by means of the following modules:

- *A motion feature extractor robust against human actions*: Using the motion signals of acceleration and angular velocity, ELESON separates the deep features of pedestrian conveyor states from human actions. Previous related studies on feature extraction require precise labels on human actions [11–14], and cannot be extended to our case due to the vast diversity of arbitrary human actions. We propose a motion feature extractor to learn the causal features from the motion signals that reflect the transportation patterns of elevators and escalators, which is independent of human actions.
- *A magnetic feature extractor to enhance estimation accuracy using magnetic field*: The magnetic signal changes differently over time for one moving in elevators and escalators. In order to mitigate the impact of local environment on magnetic signals, and observing that elevator and escalator exhibit distinct transport speeds, we propose a magnetic feature extractor to learn the more environmentally independent speed feature of elevator and escalator by means of the temporal variation of magnetic signals. As human actions, such as waving or rotating phones, may perturb the field pattern of the conveyor, the extractor further leverages adversarial learning to make the estimation more robust against arbitrary human actions.

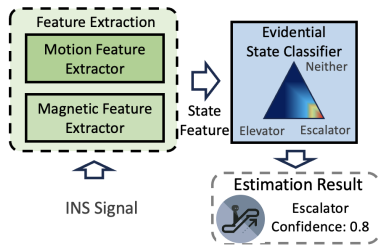


Figure 1: System overview of ELESON.

- *An evidential state classifier to estimate the conveyor state confidence:* After the motion and magnetic feature extractors, ELESON employs an evidential state classifier that estimates the confidence of pedestrian conveyor states, scoring from 0 to 1. Compared with the conventional Softmax-based classifier, our proposed classifier assesses the state confidence based on its familiarity with the target operating environment (unusual human actions, extreme magnetic environments, special conveyors, etc.) given the source training data, which enables stronger discriminability of confidence.

Figure 1 overviews the decision process of ELESON. It first extracts state features using the motion and magnetic feature extractors. With the results of the extractors, it effectively computes the confidence of pedestrian conveyor states using the evidential state classifier. Finally, the pedestrian is classified in the state of the highest confidence if the score is above a certain threshold, or “undecided” (UD) otherwise.

We have conducted extensive experiments with over twenty hours of real data, where pedestrians took different elevators and escalators with arbitrary (unknown) human actions. We compare ELESON with INS-based state-of-the-art approaches that mingle human actions with conveyor states. Our results show that ELESON outperforms significantly, achieving 15% improvement in F1 score and stronger confidence discriminability with 10% increase in AUROC (Area Under the Receiver Operating Characteristics). Furthermore, we have implemented ELESON on Android phones. ELESON operates on smartphones in real-time with low computational overhead, requiring only 9MB memory usage, and consuming less than 2% battery for an operation of 2.5 hours.

The remainder of this paper is organized as follows. We first review related work in Section 2. Then, we introduce the feature extractors and state classifier of ELESON in Sections 3 and 4, respectively. We present illustrative experimental results in Section 5, and conclude in Section 6.

2 RELATED WORK

2.1 Human Action Recognition Using Inertial Navigation System

Much work has been done on human action recognition given the signals of acceleration and angular velocity. They primarily focus on feature extraction to represent human actions.

Early works handcraft features in order to recognize human actions. For example, standing and sitting are often identified by

inactive motion signals [15, 16]; walking and ascending/descending stairs are recognized by motion intensity and cyclic features [17, 18]. More handcrafted features can be found in [16, 19]. Despite the abundant studies, such handcrafted features cannot be extended to tackle general or complex human actions in reality.

Recent studies adopt deep learning approach and investigate different model structures for human action recognition. For example, convolutional neural network has been used to extract the translation-invariant feature of human actions [20, 21], and recurrent neural network has been used to capture the long-time dependency of INS signals [22, 23]. Other model structures are discussed in [24]. While promising, the features extracted by these deep learning models are accurate in only scenarios similar to the training ones. Extracting the features of the conveyor states with these approaches is susceptible to error due to its mingling with unpredictable arbitrary human actions (validated in our experimental study section).

Recognition robustness against scenario changes has been studied for human actions. Treating phone carriage as prior knowledge, some works enhance recognition accuracy by model selection [25, 26]. Others directly tackle the feature discrepancy (such as change in users and devices) by bridging it using the training data labeled by the scenarios [7, 12–14, 27, 28]. These approaches, however, cannot be applied for our conveyor state problem because the diversity and unpredictability of human actions are difficult to either exhaustively enumerate or precisely annotate. ELESON addresses the issue by extracting causal features [29] of conveyor states from motion signals, and speed features using magnetic signals. This enhances the classification accuracy, and is free from the extra laborious effort for enumerating or labeling human actions.

2.2 Confidence Estimation for Classification Task

Confidence is the level of certainty of an object in a particular state. Sample-based approach assesses the confidence through the divergence among a group of estimates [30, 31]. Ensemble approach employs multiple classifiers to predict from an input, where a low prediction variance among the classifiers indicate high confidence [32, 33]. Bayesian neural network [31, 34, 35] and Laplacian approximation [36, 37], on the other hand, evaluate prediction variance over parameter distribution. Though promising, these approaches are computationally and resource intensive, and hence challenging its application on smartphones.

Learning-based approach assesses confidence by learning from a classifier’s previous performance. Works in [38, 39] learn an error model by evaluating the classifier under various scenarios. Free from extra networks, works in [37, 40, 41] learn classification confidence in a single model inference. While working well in a target domain similar to the testing one, these approaches tend fail with confusing confidence if operating under a different domain with pedestrian conveyor. Furthermore, their learning nature demands much training data, hampering its ease of deployment in reality.

The conventional Softmax-based classifier assesses confidence by its relative belief in the label classes, which could be overconfident or in error for a different target domain from the training one [30, 42]. Evidence approach regards training data as evidence

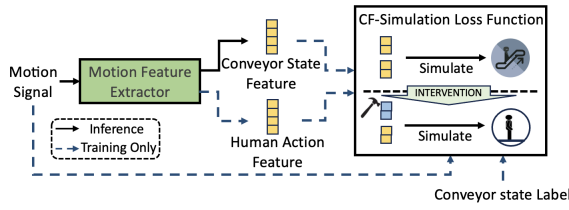


Figure 2: System diagram of motion feature extractor.

to estimate the confidence [42–44], where an underrepresented input signal is considered as a lack of evidence. In this paper, we assess state confidence by forming evidence based on the causal and temporal features of the conveyor state, hence enhancing the classifier discriminability.

3 FEATURE EXTRACTION

This section introduces ELESON’s feature-extraction approach based on motion and magnetic signals. First, we define the problem in Section 3.1. Then, we discuss the motion feature extractor in Section 3.2, followed by the magnetic feature extractor in Section 3.3.

3.1 Problem Definition

Motion and magnetic signals could be affected by the conveyor state, human action, and magnetic environment. We present the generation process of a sequence of INS signals, denoted as $x \in \mathcal{R}^{T \times 9}$, as a sampling from a conditional distribution:

$$x \sim P(x|y, k_a, k_e), \quad (1)$$

where the conveyor y is either elevator, escalator, or neither. The variables k_a and k_e represent human action and magnetic environment. Their details will be discussed later in this section.

To accurately reflect the conveyor state independent of human action and environment, our goal is learning a feature extractor, denoted as $f_{\theta}(x) = s$, such that:

$$P(s|y, k_a, k_e) = P(s|y). \quad (2)$$

In the following, we separately introduce the feature extraction approaches based on motion and magnetic signals. In each part, we first explain how human action and magnetic environment adversely affect the classification of pedestrian conveyor state and then how to tackle the issues by leveraging the characteristics of the signals. For simplicity of discussion, this section regards the conveyor state as a binary variable, where $y = 1$ indicates that a pedestrian is taking an elevator or escalator, and $y = 0$ otherwise.

3.2 Motion Feature Extractor

Motion signal reflects a phone’s acceleration and angular velocity, which is independent of magnetic environments. Since it is affected by the conveyor state and human action, we present the generation mechanism of a sequence of motion signals, denoted as $x_m \in \mathcal{R}^{T \times 6}$, as a function

$$x_m = g_m(y, k_a, k_u), \quad (3)$$

where k_u represents other minor factors for the equation rigor.

Human action and conveyor state are loosely coupled in reality. For example, a pedestrian can perform a phone call both on and

off an escalator. Thus, human action is not reliable to indicate the conveyor state of pedestrians. Moreover, due to their entanglement in the generation mechanism, human action may confuse deep learning models to be the feature of the conveyor state. For instance, deep models may use the “typing” motion to identify the “escalator” state if users frequently text on escalators in the training data, which may cause an error when a pedestrian is not texting while on an escalator. Therefore, we need to separate human action from the decision process of classifying conveyor states.

As shown in Figure 2, we propose a motion feature extractor to mitigate the model’s dependence on human action. Overall, it decomposes each sequence of motion signals into a conveyor state feature and a human action feature such that the conveyor feature is not supposed to be affected by human actions. However, this decomposition may not be straightforward because human action entangles with the conveyor state at the moment when the INS signals are generated. To tackle this, we propose a counterfactual simulation loss function that supervises the extractor to learn the decomposition.

When a pedestrian is taking an elevator or escalator, it changes the phone’s location and generates patterns in motion signals. The signal pattern is called the causal feature because it is physically generated by the conveyor, thus can reliably indicate the conveyor state of pedestrians independent of human actions. This causal feature needs to be captured by an interventional experiment, which collects and compares data in pairs. Specifically, if we are able to collect a pair of data whose conveyor state is different while strictly maintaining the same human action, the signal difference between the pairs, denoted as Δx_m , is the causal feature of conveyor state.

Based on this idea, we design an interventional experiment to extract the causal feature

$$\Delta x_m = g_m(y, k_a, k_u) - g_m(y = 0, k_a, k_u). \quad (4)$$

In particular, if y in Equation 4 is either the “elevator” or “escalator” state, the signal difference Δx_m indicates the presence of an elevator or escalator. Otherwise, Δx_m is straightforwardly a zero vector. In this way, we can learn a feature extractor to obtain the causal features of conveyors from motion signals.

However, the interventional experiment is difficult, if not impossible, to conduct by large. Alternatively, observational data, where users freely perform human actions, are typically available. To extract the causal feature using observational data, our key idea is to simulate an interventional experiment in feature space.

We rewrite Equation 4 as:

$$g_m(y, k_a, k_u) = \Delta x_m + g_m(y = 0, k_a, k_u), \quad (5)$$

which suggests that there exists a way of decomposition for obtaining the causal feature. Therefore, instead of directly extracting the causal features, we learn a motion feature extractor to decompose the motion signal:

$$f_{\theta_m}(x_m) = [s_e, s_a], \quad (6)$$

where the features s_e and s_a separately encode the information of Δx_m and $g_m(y = 0, k_a, k_u)$. We name s_e as the conveyor state feature because it encodes Δx_m . We refer to s_a as the human action feature because $g_m(y = 0, k_a, k_u)$ is dominantly affected by human

actions. However, the decomposition is nontrivial to learn without ground truth. We tackle this by using three loss functions as constraints to alternatively supervise the learning process.

First, the decomposition should not cause information loss. In other words, the decomposed features should be able to reconstruct the original signals. To achieve this, we learn a signal generator, denoted as $q_{\theta_g}(\cdot)$, to reconstruct the signal sequence using the decomposed features:

$$\mathcal{L}_{rec}(\theta_m, \theta_g) = \sum_{x_m \in \mathcal{D}} \left\| q_{\theta_g}(s_e + s_a + \sigma) - x_m \right\|_n, \quad (7)$$

where \mathcal{D} is the training dataset, $s_e + s_a$ is point-wise addition between the two features, and we additionally use a Gaussian noise $\sigma \sim \mathcal{N}(0, \Sigma^2)$ to model the minor factors in Equation 3.

Second, the conveyor state feature should causally link to the presence of an elevator and escalator. In other words, the decomposed features should properly reflect an intervention. To achieve this, we conduct an intervention on the conveyor state in the model training. Specifically, for a sequence of signal sampled from an elevator or escalator, denoted as $x_m = f(y = 1, k_a, k_u)$, we change the conveyor from elevator or escalator to neither and generate signals:

$$f(\text{do}(y = 1), k_a, k_u) = x'_m, \quad (8)$$

where $\text{do}(\cdot)$ is the do-calculus that indicates an intervention. If the decomposition is causal, the generated signals should only reflect human actions and thus conform to the signal distribution of the “neither” class:

$$x'_m \sim P(x_m | y = 0). \quad (9)$$

Based on this idea, we simulate the intervention by removing the conveyor state feature s_e and let the human action feature s_a to generate the signals whose label is “neither”:

$$q_{\theta_g}(s_a) \sim P(x_m | y = 0). \quad (10)$$

To determine whether the generated signals conform to the “neither” distribution, we employ a classifier, denoted as $r_{\theta_r}(\cdot)$, that learns to classify the conveyor state based on the decomposed feature. We summarize the simulated intervention experiments as an intervention loss function:

$$\mathcal{L}_{int}(\theta_m, \theta_r) = \sum_{(x_m, y) \in \mathcal{D}} \text{CE}(r_{\theta_r}(s_e + s_a), y) + \text{CE}(r_{\theta_r}(s_a), y = 0), \quad (11)$$

where the loss function neglects the signal generation process, and $\text{CE}(\cdot)$ represents the cross-entropy loss function.

Third, the conveyor state feature should be robust to human actions. Since we do not have labels for human actions, there are still multiple ways of decomposition even if Equation 10 is satisfied. To address this issue, we extend the concept of Sparse Mechanism Shift [29], which suggests that feature changes are typically sparse and localized within a causal decomposition. In our case, human action should not affect the process by which elevators and escalators generate the conveyor state feature. Thus, we leverage the consistency of the conveyor state feature as a constraint to learn the decomposition:

$$\mathcal{L}_{con}(\theta_m) = \sum_{(x_m, y) \in \mathcal{D}} \|s_e - \bar{s}_e\|_n, \quad (12)$$

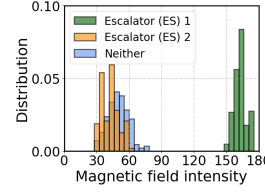


Figure 3: Magnetic field in-

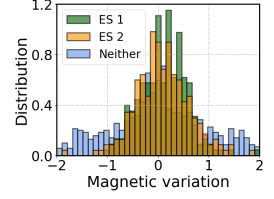


Figure 4: Temporal variability in different environments. Figure 4: Temporal variation feature to characterize the conveyor state.

where \bar{s}_e is the mean vector of the conveyor state feature over the training dataset.

Finally, we combine the three constraints by weights to be a counterfactual simulation (CF) loss function:

$$\mathcal{L}_{CF-sim} = \mathcal{L}_{int} + w_1 \mathcal{L}_{rec} + w_2 \mathcal{L}_{con}, \quad (13)$$

which supervises the learning process of motion feature extractor.

3.3 Magnetic Feature Extractor

The magnetometer samples the 3D magnetic field orientation at the phone’s location, generating a sequence of magnetic signals over time:

$$x_c = [x_c^{(0)}, x_c^{(1)}, \dots, x_c^{(T-1)}]. \quad (14)$$

Elevator and escalator affect magnetic signals by changing the phone’s location mediated via the pedestrian, which enables the estimation of conveyor state.

However, the magnetic signals also depend on the magnetic field of the local environments. The signal distribution, as shown in Figure 3, may significantly differ when taking elevators and escalators at different locations, making it difficult to obtain a stable representation of the conveyor state across various environments. Furthermore, humans may perform various actions, such as waving and rotating phones, that causes fluctuations in the magnetic signals. This has complicated and adversely diversified the signal patterns of the conveyor state, making the classification prone to errors.

To tackle these issues, we propose a magnetic feature extractor to obtain the conveyor state feature decoupled from human action and environment. As shown in Figure 5, it uses a variation feature extractor to obtain the conveyor features that apply to different environments and employs an action filter to reduce the human-action impacts on the feature. In the training process, the action filter learns from an action-adversarial loss function.

To introduce the extractor design, we first consider that a phone is relatively stationary with a pedestrian; that is, the pedestrian does not perform any action to fluctuate the phone’s location. In this scenario, the location change of the phone is fully due to the elevator or escalator. Hence, the speed feature of the conveyors can be reflected by the temporal variation of magnetic field. Since the speed feature is much more stable than magnetic signal distributions in different environments, we use the temporal variation of magnetic field, i.e. magnetic variation, to characterize the conveyor states.

To further support this idea, we conduct an experiment to visualize and compare the magnetic field intensity and magnetic variation in Figure 3 and Figure 4. In the figures, magnetic variation not only

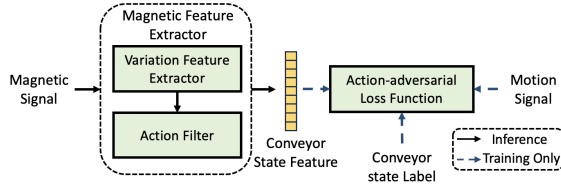


Figure 5: System diagram of magnetic feature extractor.

differentiates the conveyor states but also is more consistent in different operating environments than magnetic field intensity. Based on this observation, we propose a variation feature extractor to extract the variation feature from magnetic field intensity:

$$\Delta x_c = f_v(x_c) = \left[\left\| x_c^{(t)} \right\|_2 - \left\| x_c^{(t-1)} \right\|_2, t = 1, 2, \dots, T \right]. \quad (15)$$

Nevertheless, human actions may fluctuate the phone's location and perturb the variation feature. To tackle this, we propose an action filter that enhances the variation feature to be insensitive to human actions:

$$f_{\theta_c}(\Delta x_c) = s_c. \quad (16)$$

Specifically, we regard the signal fluctuation caused by human actions as noises and extract a feature that is invariant to them:

$$P(s_c | y = 1, k_a = 0) = P(s_c | y = 1, k_a = 1), \quad (17)$$

where $k_a = 1$ refers to the human action that perturbs magnetic signals such as waving, and $k_a = 0$ otherwise.

We learn the action filter through adversarial learning because human action is independent of the magnetic environment in practice. Specifically, the filter plays a min-max game with a classifier, denoted as $f_{\theta_b}(\cdot)$, that tries to classify k_a using magnetic signals:

$$\min_{\theta_b} \max_{\theta_c} \sum_{x_c \in \mathcal{D}} \text{CE}(f_{\theta_b}(s_c), k_a). \quad (18)$$

We determine k_a by a threshold of angular velocity, where the signal whose angular velocity is larger than the threshold is automatically labeled as $k_a = 1$. This is based on the observation that human actions usually can generate large angular velocities while elevators and escalators cannot.

Overall, we concatenate the conveyor state features extracted from the motion and magnetic signals as a state feature:

$$s = \text{CONCAT}(s_e, s_c), \quad (19)$$

which is used to classify the conveyor state in Section 4.

4 EVIDENTIAL STATE CLASSIFIER

After the feature extractors discussed in Section 3, ELESON employs an evidential state classifier to estimate the state confidence of pedestrians. In Section 4.1, we overview the conveyor state classification based on the feature extractors, followed by the technical details of the design in Section 4.2.

4.1 Overview

The conveyor state of elevator and escalator has causal features and sequential features. The causal features, as discussed in Section 3, are the motion and magnetic variation of INS signal patterns, which

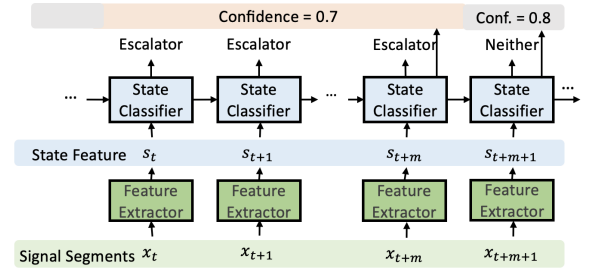


Figure 6: Illustration of the conveyor state estimation based on temporal signals.

are physically correlated with the presence elevators and escalators. The sequential feature refers to the typical orders in which human actions and causal features usually appear. For example, a pedestrian has to get on an escalator before stepping off. Clearly, both of the features are useful for classifying the conveyor state of pedestrians.

Due to the varying duration of pedestrians using elevators and escalators, ELESON adopts a flexible model structure to capture the causal features and sequential features, which is illustrated in Figure 6. First, the feature extractors extract the state features from segments of signals (say, of two-second length). Then, the state classifier captures the feature sequence to classify the conveyor state of each segment. The whole system can work in real time.

In practice, the classification system needs to handle various operating environments, such as various types of conveyors, unusual human actions, extreme magnetic environments, and so on. To account for the variety of environments, we design the state classifier to estimate the state confidence of pedestrians, where the classification decision is made upon the state with the highest confidence:

$$\hat{y} = \arg \max_{y \in \mathcal{Y}} b_y, \quad (20)$$

where b_y is the classifier's confidence of the state y , and $\mathcal{Y} = \{EL, ES, N\}$. While, if the confidence in the decision is lower than a threshold, the system would suggest an "undecided" (UD) classification result.

We estimate the confidence based on the causal features and sequential features. On the one hand, the classification may not be very confident if the classifier is unfamiliar with the state features. On the other hand, it may indicate large uncertainty if the sequence of state features violates the sequential feature of the conveyor state. For example, it is unlikely for a pedestrian to get off an escalator before stepping on. Therefore, as shown in the figure, the classifier estimates confidence over the sequence of state features if the signal is classified as elevator or escalator. Otherwise, the classifier directly estimates the state confidence.

4.2 Design Details

The design of the evidential state classifier is shown in Figure 7. It first captures the sequential feature of conveyor state using a sequential feature extractor. Then, it collects evidence from the sequential feature using an evidence collector. Finally, confidence

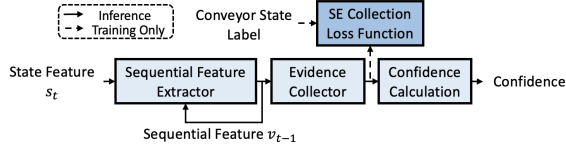


Figure 7: System diagram of evidential state classifier.

is assessed from the collected evidence through a module of confidence calculation. In the training stage, the classifier learns from a sequential evidence (SE) collection loss function.

The sequential feature extractor is designed to capture the causal features and sequential features of the conveyor state, based on the feature extractors mentioned in Section 3:

$$k_{\omega_v}(s_t, v_{t-1}) = v_t. \quad (21)$$

We empirically build the extractor based on LSTM [45], while other sequential models should be suitable as well.

Given the sequential feature, we aim to estimate the confidence of the pedestrian in each of the conveyor states. Intuitively, a proper confidence score should be informative of misclassification. In this paper, we estimate the confidence by considering state ambiguity and signal unfamiliarity.

State ambiguity refers to the issue that an input signal has the features of multiple states. For example, since elevator and escalator barely cause phones' rotation, the low intensity of angular velocity can indicate either elevator or escalator. Softmax-based classifier captures the state ambiguity by classification scores. For instance, the classification scores of "[EL=0.8, ES=0.2, N=0.]" means that the input signals are more likely to be classified as "elevator" than "escalator", while being impossible to be "neither".

Signal unfamiliarity describes how much evidence in which a classifier has for processing the input signal. While the state ambiguity concerns with the relative confidence among the conveyor states, signal unfamiliarity expresses the subjective confidence of the classifier given its training data. For example, if a pedestrian performs some actions that have not been represented in training data (say, performing a ballet), the classification itself is uncertain, no matter of the relative confidence among the states.

To account for the state ambiguity and signal unfamiliarity, the classifier assigns its confidence to a simplex of the space of conveyor states:

$$u + \sum_{y \in \mathcal{Y}} b_y = 1, \quad (22)$$

where the relative confidence among b_y represents the state ambiguity, and u represents the degree to which the classifier is unfamiliar with the input signal.

From the perspective of a frequentist, unfamiliarity can be interpreted as a low frequency of a classifier learning to process an input signal. In other words, a classifier tends to be more confident, and more accurate, in classifying an input signal when it encounters the signal more frequently in the training data. Hence, the learning experiences can be regarded as evidence to support the confidence of each state. Thus, we build an evidence collector to assess evidence from the sequential feature:

$$k_{\omega_e}(v_t) = e_t. \quad (23)$$

whose last layer is ReLU [46] because the evidence quantity should be non-negative.

Based on the evidence of each state, we estimate the confidence through a normalization, named confidence calculation:

$$b_y = \frac{e_y}{\sum_{y' \in \mathcal{Y}} e_{y'} + k}, \quad (24)$$

where e_y is the amount of evidence of state y , and k is a constant mass reserved for unfamiliarity (usually, $k = |\mathcal{Y}|$):

$$u = \frac{k}{\sum_{y' \in \mathcal{Y}} e_{y'} + k}. \quad (25)$$

As an example, if the classifier has not seen an input signal under any of the states, i.e. $\sum_{y' \in \mathcal{Y}} e_{y'} = 0$, the unfamiliarity term would occupy all confidence masses, i.e. $u = 1$.

The goal of the evidence collector is to extract more evidence when the input signal is well-represented in the training data. To achieve this, we learn the evidence collector based on a transformation. Specifically, the simplex in Equation 22 is equivalent to a Dirichlet distribution, where evidence can be used to calculate the prior parameters of the distribution (proof can be found in [43]):

$$\alpha_y = e_y + 1. \quad (26)$$

The relative confidence assignment in Equation 22 can be interpreted as the distribution's expectation:

$$\mathbb{E}_\alpha(y) = \frac{\alpha_y}{A} = \frac{b_y + 1}{\sum_{y \in \mathcal{Y}} (b_y + 1)}, \quad (27)$$

where $\alpha \in [\alpha_{EL}, \alpha_{ES}, \alpha_N]$, and $A = \sum_{y \in \mathcal{Y}} \alpha_y$; a lack of evidence to support a state is equivalent to a large variance in the distribution:

$$\text{Var}(y) = \frac{\alpha_y(A - \alpha_y)}{A^2(A + 1)}. \quad (28)$$

In simple terms, learning to classify conveyor state is equivalent to optimizing the expectation of the Dirichlet distribution, and learning to collect evidence is to minimizing the distribution variance.

Based on the transformation, we learn the evidential state classifier using a sequential evidence (SE) collection loss function:

$$\mathcal{L}_{SE}(\omega_v, \omega_e) = \sum_{Q \in \mathcal{D}} \sum_{(x_t, y_t) \in Q} \left(\left(y_t - \frac{\hat{\alpha}_t}{\hat{A}_t} \right)^2 + z(y_t) \sum_{y \in y_t} \text{Var}(y) \right). \quad (29)$$

For each sequence of INS signals Q from the training dataset \mathcal{D} , we optimize the expectation on each signal segment from the sequence. To capture the sequential feature to estimate confidence, we regard the complete sequence of state features as evidence and only optimize the distribution variance when the conveyor state is neither or at the end of the elevator and escalator states, which is implemented by an indicator function:

$$z(y_t) = \begin{cases} 1, & y_t = N \text{ or } t = t_{end}, \\ 0, & \text{Otherwise,} \end{cases} \quad (30)$$

where t_{end} labels the segment at pedestrians ending an elevator or escalator state. For instance, if the state features show that a pedestrian step off an escalator before getting on, this would generate a sequential feature that is out of distribution of the training data, which leads to a low confidence.

Table 1: F1 score under different phone carriage styles.

Carriage style	Reading	In-pocket	Hand-swinging	In-bag
Handcraft	0.73	0.61	0.69	0.58
ConvLSTM	0.76	0.76	0.68	0.77
MD (Rand)	0.79	0.75	0.71	0.73
DIVERSITY	0.79	0.75	0.72	0.78
MD (Label)	0.80	0.78	0.72	0.77
ELESON	0.92	0.92	0.83	0.88

5 ILLUSTRATIVE EXPERIMENTAL RESULTS

In this section we evaluate the performance of ELESON. We first discuss the experimental settings in Section 5.1, and then present illustrative results in Section 5.2.

5.1 Experimental Setting

We collected the first dataset for the classification of pedestrian conveyor state to validate ELESON. In each data collection, a phone user decides whether to take an elevator or escalator and can freely perform any actions. In the meantime, an observer annotates the conveyor state of the phone user and precisely records the timestamps whenever he/she gets on and off an elevator or escalator. Overall, we have collected twenty hours of INS signals from fifteen users, with twelve hours of data on different elevators and escalators from ten shopping malls.

We validate ELESON on the collected time-series signals and report estimation results every two seconds. Considering that users stay shorter time on elevators and escalators than elsewhere, we evaluate the classification accuracy by F1 score individually for elevator and escalator classes (e.g., elevator is regarded as negative when evaluating F1 score for escalator):

$$\text{F1 score} = \frac{2 \times \text{Precision} \times \text{Recall}}{\text{Precision} + \text{Recall}}, \quad (31)$$

where precision and recall are the proportions of true positives separately over predicted positives and actual positives:

$$\begin{aligned} \text{Precision} &= \frac{\text{TP}}{\text{TP} + \text{FP}}; \\ \text{Recall} &= \frac{\text{TP}}{\text{TP} + \text{FN}}. \end{aligned} \quad (32)$$

In the equations, TP, FP, and FN separately stand for “true positive”, “false positive”, and “false negative”.

We compare ELESON with state-of-the-art approaches of human action recognition and robust feature extraction:

- *Action-feature approach (Handcraft)* [47] handcrafts features of human actions that are classified by a neural network;
- *ConvLSTM* [9] is a widely adopted deep-model structure for INS-based human action recognition, which combines a convolutional neural network with LSTM;
- *Multi-domain Approach (MD)* [12] relies on scenario labels to extract robust deep features. In the experiment, we implement it by labeling human actions using phone carriage styles (as shown in Table 1) and additionally show its performance with random grouping (rand);

- *DIVERSIFY* [7] conducts multi-domain approach by pseudo labels, where human actions are labeled and grouped by exploring the signal correlations in training data.

We verify confidence estimation by the area under the receiver operating characteristic curve (AUROC), which measures the confidence’s discriminability to distinguish correct and false classification results. In particular, we regard it as a true positive case when a false classification (or decision) is discarded as UD. Thus, AUROC measures the trade-off between false positive rate (FPR) and true positive rate (TPR):

$$\text{AUROC} = \int \text{TPR}(\text{FPR}) d\text{FPR}. \quad (33)$$

We compare confidence estimation with the following approaches:

- *Entropy approach (Softmax)* [46] uses information entropy of the classification score to presents the confidence of Softmax-based classifier;
- *Bayesian neural network (Bayesian)* [35] represents confidence using prediction variance over network parameter’s distribution. In the experiment, we sample network parameter by Dropout mechanism [46];
- *Temperature scaling (TempScale)* [41] calibrates the classification scores using an exponential parameter determined by the classifier’s performance in training data and calculates confidence using the information entropy of the scores.

To verify ELESON’s on-device performance, we have deployed it to an Android phone (Huawei LDN-AL10) and investigated its power consumption, memory usage and inference time. Additionally, we verified the on-device accuracy of ELESON through a crowdsourcing experiment, where several users downloaded ELESON to their smartphones and evaluates it by roughly estimating the time slots (around two minutes) when they were taking an elevator or escalator. In particular, we regard it as a true positive case if an “elevator” or “escalator” is reported in the time slots and report the classification accuracy by F1 score. Overall, the crowdsourced experiment includes one hour of signals on elevators and escalators.

In the experiment, the learning of ELESON is optimized by Adam optimizer in an end-to-end manner. For the modules mentioned in Section 3 and 4, we empirically use four fully connected layers with ReLU functions unless particularly specified. The conveyor state features of motion and magnetic signals have 128 dimensions. To reduce randomness, each experiment is repeated five times, where the average results are reported.

5.2 Illustrative Results

1) *System setup*: This part demonstrates how the ELESON’s modules contribute to the model performance. Each figure demonstrates the module setup that builds upon the previous one. Unless particularly specified, we use 80% data for training and the left for testing.

Figure 8 verifies the reconstruction loss function in Equation 7. It shows how accuracy varies with the weight of the loss function (based on the intervention loss function in Equation 11). From the figure, the accuracy increases when the weight is less than 0.4 because the reconstruction loss function reduces the information loss of decomposition. However, the accuracy may slightly decrease

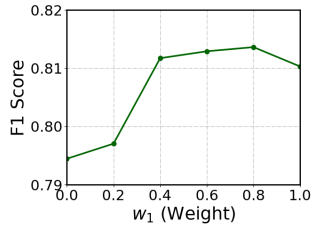


Figure 8: Verification on reconstruction loss function.

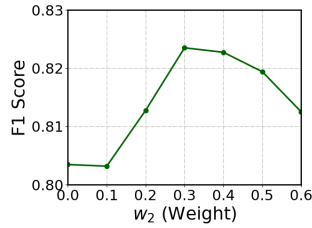


Figure 9: Verification on consistency loss function.

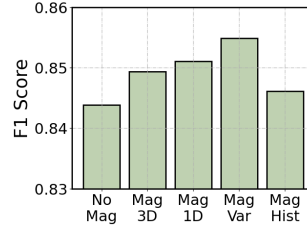


Figure 10: Comparison of the features of magnetic field.

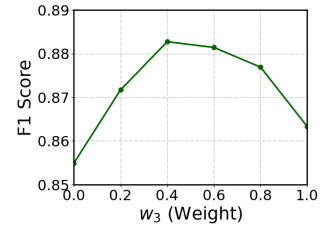


Figure 11: Accuracy by introducing the action filter.

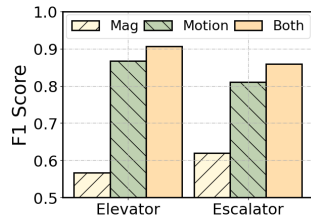


Figure 12: Ablation study on the two feature extractors.

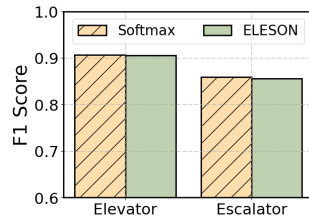


Figure 13: Accuracy comparison of classifiers.

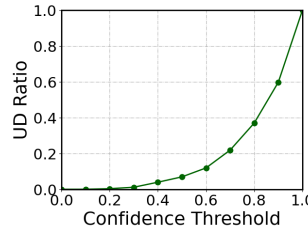


Figure 14: UD (undecided) ratio varies with threshold.

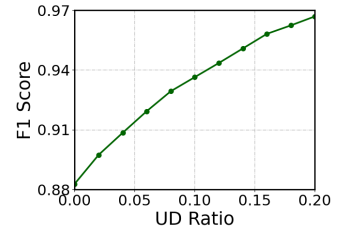


Figure 15: Accuracy varies with UD ratio.

if w_1 is too large (> 0.8) since it deviates the training objective. In the experiment, we use $w_1 = 0.6$.

Figure 9 verifies the consistency loss function as in Equation 12. In the figure, the accuracy shows a U-shape as the weight of the loss function increases. The accuracy increase is because the consistency loss function stabilizes the causal feature. The accuracy decrease, on the other hand, is when the weight is so large that the extracted features are inflexible. In the experiment, we use $w_2 = 0.3$.

Figure 10 compares different features extracted from magnetic signals. “Mag3D” stands for the 3D magnetic orientation, “Mag1D” is the magnetic field intensity, “Mag Var” is the sequence of magnetic variation, and “Mag Hist” is the histogram of the magnetic variation. Although all features enhance the classification accuracy by introducing magnetic signals, the magnetic variation outperforms other features by a large margin because it captures the transport speed of elevators and escalators.

Figure 11 shows the accuracy by introducing the action filter, where w_3 is the weight of the adversarial learning in Equation 18. Similar to the consistency loss function, the accuracy shows a U-shape varying with the weight. The accuracy increases because the action filter tackles the signal fluctuation caused by human actions. However, stressing too much on adversarial learning may render the feature inflexible. In the experiment, we use $w_3 = 0.4$.

Figure 12 shows how the motion and magnetic feature extractors contribute to the classification accuracy. When independently applied, the motion feature extractor is more accurate than the magnetic feature extractor because the feature of the conveyor state is more prominent and stable in motion than magnetic signals. Despite so, the magnetic feature extractor enhances the classification accuracy based on the motion feature extractor, because it captures the speed feature of the conveyor state.

Based on the feature extractors, Figure 13 compares the classification accuracy of the softmax-based classifier and evidential state classifier. Although the approach accuracy regarding the elevator state is slightly higher than that of the escalator state, the accuracy differences of both states are insignificant. This is because the evidential state classifier jointly learns classification as well as confidence estimation in the training process.

By showing the ratio of the undecided (UD) cases varies with the confidence threshold, Figure 14 demonstrates the confidence distribution of ELESon in the real-world scenarios (verified on the whole dataset via cross-validation). From the figure, the confidence distribution shows a short tail on the left side, suggesting that ELESon is confident about most of its decisions. In particular, around 95% of decisions are confident if pinning 0.5 as a threshold.

A higher confidence threshold renders more model predictions being discarded as undecided cases (UD). Figure 15 demonstrates how the accuracy of confident decisions varies with the UD ratio. From the figure, the curve shows a convex shape with an extremely high accuracy based on a low UD ratio of 0.2. This has validated that the confidence of ELESon can effectively imply decision accuracy.

2) *Scheme comparison*: This part compares the schemes’ performance on the twenty hours of data via five-fold cross-validation.

We set 0.5 as the confidence threshold (leading to 5% UD cases) and compare ELESon with existing schemes mentioned in Section 5.1. From the figure, the low F1 score of Handcraft is because human actions are loosely coupled with the conveyor state of pedestrians. Perturbed by human actions, all previous schemes cannot balance recall and precision because they train and infer by treating INS signals as an aggregate. In comparison, ELESon achieves satisfied results on recall and precision because it decouples the conveyor state from human actions in feature space. Overall, ELESon outperforms previous works by around 15% in F1 score averagely.

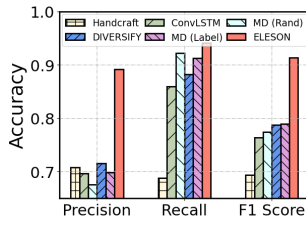


Figure 16: Comparison on classification accuracy.

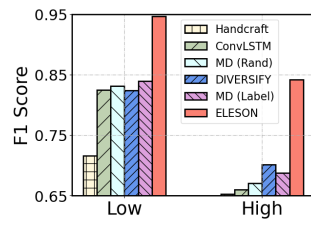


Figure 17: Accuracy varies with levels of action perturbations.

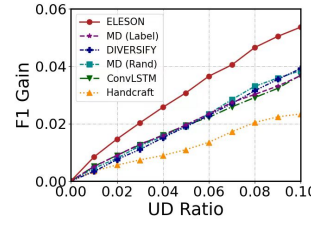


Figure 18: F1 gain varies with UD ratio.

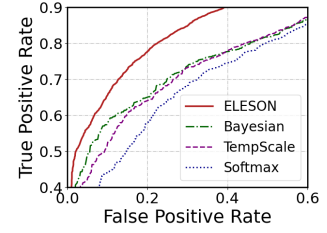


Figure 19: ROC of identifying false decisions.

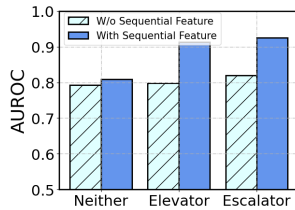


Figure 20: Verification of SE collection loss function.

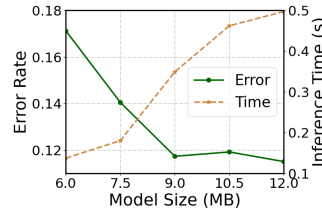


Figure 21: Inference time varies with model size.

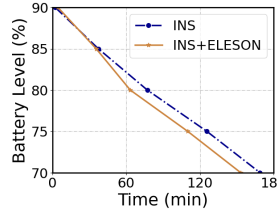


Figure 22: Power consumption on a smartphone.

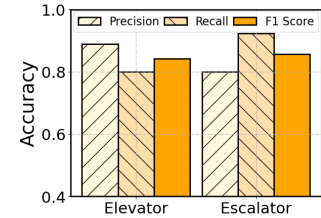


Figure 23: On-device accuracy based on crowdsourced data.

Figure 17 compares the scheme accuracy with and without significant perturbations of human actions. As mentioned in Section 3.3, we use an intensity threshold (of 3.0) on angular velocity to differentiate the action perturbation on INS signals. From the figure, the accuracy of all schemes, including ELESON, degrades when dealing with significant perturbations. This is unavoidable because the action perturbation reduces the signal-to-noise ratio in both motion and magnetic signals. While the performance of previous works fluctuates significantly with various operating environments, ELESON maintains a high accuracy of over 84% in either scenario.

Table 1 further compares the scheme accuracy under different phone carriage styles, which is a coarse and explainable way to classify human actions. From the table, ELESON shows superior accuracy over the comparison schemes, which is consistent with the previous results. Note that, it even outperforms MD with carriage-style labels by a large margin because the causal decomposition is more effective than the coarse label of human actions.

Figure 18 demonstrates how the F1 score varies with the UD ratio (by changing the confidence threshold), where the comparison schemes use the Softmax-based classifier just as their original setting. Being sensitive to unfamiliar signals, ELESON acquires a significant gain in F1 score by considering confidence, while other approaches cannot discriminate between correct and false decisions because the Softmax-based classifier tends to be overconfident.

Figure 19 compares the confidence estimation of ELESON with existing approaches using the ROC curve, which indicates better discriminability of confidence by being closer to the upper-left corner. From the figure, Bayesian’s performance is affected by its sampling nature on the large parameter space, and TempScale is inflexible in calibrating the classification score. Thus, their improvement from Softmax is limited. In comparison, ELESON directly

learns to assign confidence from the causal and sequential features of the conveyor states, which is computationally efficient with a stronger discriminability in model inference. Overall, the evidence approach of ELESON demonstrates its suitability to this task by outperforming existing schemes by around 10% in AUROC.

Figure 20 compares ELESON with or without considering the sequential feature. We may consider the approach without sequential features as the vanilla evidence approach. From the figure, the AUROC in both “elevator” and “escalator” states shows a significant gain by considering the sequential feature. This has validated that the sequential feature enhances the discriminability of confidence.

3) *On-device Experiments:* This part verifies ELESON’s performance on smartphones.

Figure 21 shows how accuracy and single-inference time vary with model sizes. In the experiment, we adjust the model size by proportionally changing the neuron quantity of each layer. From the figure, as the model size grows, the error rate reduces, and inference time increases. Using the knee point of the accuracy curve as model size (9MB, 0.3% of the smartphone’s memory) each inference takes 0.4 seconds. This has verified the real-time performance and the minimal memory usage of ELESON in a real-world deployment.

Figure 22 demonstrates the power consumption by running ELESON on a smartphone. From the figure, INS consumes around 18% of the battery power (from 90% to 72%) in 150 minutes, while additionally running ELESON only takes more 2% in the same period. This shows ELESON’s minimal computational cost in terms of power consumption.

Figure 23 shows the on-device accuracy of ELESON based on the crowdsourced data. From the figure, ELESON’s accuracy on crowdsourced data is comparable with our previous results. This has validated ELESON’s high accuracy in more real-world scenarios.

6 CONCLUSION

We investigate, for the first time, how to classify a pedestrian in one of the three conveyor states of elevator, escalator and neither, given the INS readings of acceleration, angular velocity and magnetic fields sampled from the pedestrian's phone. Previous studies on human action recognition (HAR) cannot be extended to our problem with satisfactory results because the INS signals of the conveyor state is entangled by unpredictable, arbitrary and diverse human actions. We propose ELESON, a novel lightweight INS-based deep learning approach to classify pedestrian to elevator, escalator or neither. ELESON utilizes a motion feature extractor to decouple the conveyor state from human action in feature space, and a magnetic feature extractor to learn the speed features of elevator and escalator. Given the results of the two extractors, it uses an evidential state classifier to effectively estimate the state confidence of the pedestrian. We have conducted experiments to validate ELESON on over twenty hours of real pedestrian data and compared it with state-of-the-art HAR approaches (where INS signals of both the conveyor state and human actions are processed together). Our results show that ELESON outperforms significantly, improving 15% in F1 score and increasing 10% confidence discriminability in AUROC. Furthermore, we have implemented ELESON on Android phones. ELESON operates on smartphones in real-time with low computational overhead, requiring only 9MB memory usage and consuming less than 2% battery with an operation of 2.5 hours.

In our future work, we plan to incorporate domain generalization approaches to consider user and device heterogeneity. This enhancement is orthogonal to the contribution of this paper, but it will further enhance the system performance. Additionally, being the first to consider the conveyor states of pedestrians using smartphones, we will extend its applicability to more conveyors such as travelators, wheelchairs, self-balancing scooters, etc.

REFERENCES

- [1] H. et al., "MM-Tap: Adaptive and Scalable Tap Localization on Ubiquitous Surfaces with mm-level Accuracy," *IEEE IoTJ*, 2023.
- [2] —, "Self-Supervised Association of Wi-Fi Probe Requests Under MAC Address Randomization," *IEEE Transactions on Mobile Computing*, 2022.
- [3] H. Ma, Y. He, M. Li, N. Patwari, and S. Sigg, "Introduction to the Special Issue on Wireless Sensing for IoT," pp. 1–4, 2023.
- [4] Z. et al., "FIS-ONE: Floor Identification System with One Label for Crowdsourced RF Signals," in *ICDCS 2023*, 2023, pp. 418–428.
- [5] J. Tan, H. Wu, K.-H. Chow, and S.-H. G. Chan, "Implicit Multimodal Crowdsourcing for Joint RF and Geomagnetic Fingerprinting," *IEEE Transactions on Mobile Computing*, vol. 22, no. 2, pp. 935–950, 2023.
- [6] R. Vrskova, P. Kamencay, R. Hudec, and P. Sykora, "A New Deep-learning Method for Human Activity Recognition," *Sensors*, vol. 23, no. 5, p. 2816, 2023.
- [7] W. Lu, J. Wang, X. Sun, Y. Chen, and X. Xie, "Out-of-Distribution Representation Learning for Time Series Classification," 2023.
- [8] J. e. a. Lu, "Robust Single Accelerometer-based Activity Recognition Using Modified Recurrence Plot," *IEEE Sensors Journal*, vol. 19, no. 15, pp. 6317–6324, 2019.
- [9] A.-A. et al., "Human Activity Recognition Using Temporal Convolutional Neural Network Architecture," *Expert Systems with Applications*, vol. 191, p. 116287, 2022.
- [10] H. Xu, P. Zhou, R. Tan, and M. Li, "Practically Adopting Human Activity Recognition," in *Proceedings of the 29th Annual International Conference on Mobile Computing and Networking*, 2023, pp. 1–15.
- [11] H. Li, S. J. Pan, S. Wang, and A. C. Kot, "Domain Generalization With Adversarial Feature Learning," in *CVPR*, 2018, pp. 5400–5409.
- [12] L. Chen, Y. Zhang, Y. Song, A. Van Den Hengel, and L. Liu, "Domain generalization via rationale invariance," in *CVPR*, 2023, pp. 1751–1760.
- [13] M. et al., "Spatial-Temporal Masked Autoencoder for Multi-Device Wearable Human Activity Recognition," *IMWUT*, vol. 7, no. 4, pp. 1–25, 2024.
- [14] K. et al., "Human Activity Recognition from Multiple Sensors Data Using Deep CNNs," *Multimedia Tools and Applications*, vol. 83, no. 4, pp. 10 815–10 838, 2024.
- [15] Z. Yang, C. Wu, Z. Zhou, X. Zhang, X. Wang, and Y. Liu, "Mobility Increases Localizability: A Survey on Wireless Indoor Localization Using Inertial Sensors," *ACM Computing Surveys (Csur)*, vol. 47, no. 3, pp. 1–34, 2015.
- [16] E. Bulbul, A. Cetin, and I. A. Dogru, "Human Activity Recognition Using Smartphones," in *ISMSIT*. IEEE, 2018, pp. 1–6.
- [17] A. Brajdic and R. Harle, "Walk Detection and Step Counting on Unconstrained Smartphones," in *UbiComp*, 2013, pp. 225–234.
- [18] X. Kang, B. Huang, and G. Qi, "A Novel Walking Detection and Step Counting Algorithm Using Unconstrained Smartphones," *Sensors*, vol. 18, no. 1, p. 297, 2018.
- [19] F. Demrozi, G. Pravadelli, A. Bihorac, and P. Rashidi, "Human activity recognition using inertial, physiological and environmental sensors: A comprehensive survey," *IEEE access*, vol. 8, pp. 210 816–210 836, 2020.
- [20] M. et al., "CNN-based Sensor Fusion Techniques for Multimodal Human Activity Recognition," in *ACM ISWC*, 2017, pp. 158–165.
- [21] C. et al., "Comparing CNN and Human Crafted Features for Human Activity Recognition," in *UIC-ATC*. IEEE, 2019, pp. 960–967.
- [22] K. et al., "Deep CNN-LSTM with Self-attention Model for Human Activity Recognition Using Wearable Sensor," *IEEE Journal of Translational Engineering in Health and Medicine*, vol. 10, pp. 1–16, 2022.
- [23] O. Nafea, W. Abdul, and G. Muhammad, "Multi-sensor Human Activity Recognition Using CNN and GRU," *International Journal of Multimedia Information Retrieval*, vol. 11, no. 2, pp. 135–147, 2022.
- [24] G. Saleem, U. I. Bajwa, and R. H. Raza, "Toward Human Activity Recognition: A Survey," *Neural Computing and Applications*, vol. 35, no. 5, pp. 4145–4182, 2023.
- [25] B. et al., "Comparing Handcrafted Features and Deep Neural Representations for Domain Generalization in Human Activity Recognition," *Sensors*, vol. 22, no. 19, p. 7324, 2022.
- [26] T. Shen, I. Di Giulio, and M. Howard, "A Probabilistic Model of Human Activity Recognition with Loose Clothing," *Sensors*, vol. 23, no. 10, p. 4669, 2023.
- [27] R. Hu, L. Chen, S. Miao, and X. Tang, "SWL-Adapt: An Unsupervised Domain Adaptation Model with Sample Weight Learning for Cross-user Wearable Human Activity Recognition," in *AAAI*, vol. 37, no. 5, 2023, pp. 6012–6020.
- [28] J. Yang, Y. Xu, H. Cao, H. Zou, and L. Xie, "Deep Learning and Transfer Learning for Device-free Human Activity Recognition: A Survey," *Journal of Automation and Intelligence*, vol. 1, no. 1, p. 100007, 2022.
- [29] B. Schölkopf, F. Locatello, S. Bauer, N. R. Ke, N. Kalchbrenner, A. Goyal, and Y. Bengio, "Toward Causal Representation Learning," *Proceedings of the IEEE*, vol. 109, no. 5, pp. 612–634, 2021.
- [30] G. et al., "A Survey of Uncertainty in Deep Neural Networks," *Artificial Intelligence Review*, vol. 56, no. Suppl 1, pp. 1513–1589, 2023.
- [31] Y. Gal, "Uncertainty in Deep Learning," *University of Cambridge*, 2016.
- [32] L. et al., "Simple and Scalable Predictive Uncertainty Estimation Using Deep Ensembles," *NIPS*, vol. 30, 2017.
- [33] Y. Wen, D. Tran, and J. Ba, "Batchensemble: An Alternative Approach to Efficient Ensemble and Lifelong Learning," *arXiv preprint arXiv:2002.06715*, 2020.
- [34] Y. Li and Y. Gal, "Dropout Inference in Bayesian Neural Networks with Alpha-divergences," in *ICML*. PMLR, 2017, pp. 2052–2061.
- [35] P. Thiagarajan, P. Khairnar, and S. Ghosh, "Explanation and Use of Uncertainty Quantified by Bayesian Neural Network Classifiers for Breast Histopathology Images," *IEEE transactions on medical imaging*, vol. 41, no. 4, pp. 815–825, 2021.
- [36] J. Lee, M. Humt, J. Feng, and R. Triebel, "Estimating Model Uncertainty of Neural Networks in Sparse Information Form," in *ICML*. PMLR, 2020, pp. 5702–5713.
- [37] N. et al., "Towards Maximizing the Representation Gap between In-domain & Out-of-distribution Examples," *NIPS*, vol. 33, pp. 9239–9250, 2020.
- [38] A. Malinin and M. Gales, "Predictive Uncertainty Estimation via Prior Networks," *NIPS*, vol. 31, 2018.
- [39] T. Ramalho and M. Miranda, "Density Estimation in Representation Space to Predict Model Uncertainty," in *EDSMLS*. Springer, 2020, pp. 84–96.
- [40] C. Guo, G. Pleiss, Y. Sun, and K. Q. Weinberger, "On Calibration of Modern Neural Networks," in *ICML*. PMLR, 2017, pp. 1321–1330.
- [41] A. Karandikar, N. Caim, D. Tran, B. Lakshminarayanan, J. Shlens, M. C. Mozer, and B. Roelofs, "Soft calibration objectives for neural networks," *Advances in Neural Information Processing Systems*, vol. 34, pp. 29 768–29 779, 2021.
- [42] M. Sensoy, L. Kaplan, and M. Kandemir, "Evidential Deep Learning to Quantify Classification Uncertainty," in *NIPS*, vol. 31, 2018.
- [43] A. Jøsang, *Subjective logic*. Springer, 2016, vol. 3.
- [44] J. Liu, Z. Lin, S. Padhy, D. Tran, T. Bedrax Weiss, and B. Lakshminarayanan, "Simple and Principled Uncertainty Estimation with Deterministic Deep Learning via Distance Awareness," *NIPS*, vol. 33, pp. 7498–7512, 2020.
- [45] S. Hochreiter and J. Schmidhuber, "Long Short-term Memory," *Neural computation*, vol. 9, no. 8, pp. 1735–1780, 1997.
- [46] A. Krizhevsky, I. Sutskever, and G. E. Hinton, "Imagenet Classification with Deep Convolutional Neural Networks," *NIPS*, vol. 25, 2012.
- [47] W. et al., "A Comparative Study on Human Activity Recognition Using Inertial Sensors in a Smartphone," *IEEE Sensors Journal*, vol. 16, no. 11, 2016.

Received 20 February 2007; revised 12 March 2009; accepted 5 June 2009